

See discussions, stats, and author profiles for this publication at: <https://www.researchgate.net/publication/319648258>

Vitamin D receptor-targeted treatment to prevent pathological dedifferentiation of pancreatic β cells under...

Article in *Diabetes & Metabolism* · September 2017

DOI: 10.1016/j.diabet.2017.07.006

CITATIONS

0

READS

8

6 authors, including:



[Abraham Neelankal John](#)

Harry Perkins Institute of Medical Research

4 PUBLICATIONS 13 CITATIONS

SEE PROFILE



Available online at
ScienceDirect
www.sciencedirect.com

Elsevier Masson France
EM|consulte
www.em-consulte.com



Original article

Vitamin D receptor-targeted treatment to prevent pathological dedifferentiation of pancreatic β cells under hyperglycaemic stress

A. Neelankal John^{a,b}, Z. Iqbal^d, S. Colley^{a,b}, G. Morahan^{a,b}, M. Makishima^c, F.-X. Jiang^{a,b,*}

^a Harry-Perkins Institute of Medical Research, Centre for Medical Research, University of Western Australia, Nedlands, Verdun St, Perth, 6009 Western Australia, Australia

^b School of Medicine and Pharmacology, University of Western Australia, Crawley, Western Australia, Australia

^c Division of Biochemistry, Okayama University, Graduate School of Medicine, Dentistry and Pharmaceutical Science, 2-5-1 Shikata-cho, Kita-ku, Okayama, Japan

^d Department of Chemistry, Quaid-I-Azam University Islamabad, Pakistan

ARTICLE INFO

Article history:

Received 7 March 2017
Received in revised form 20 June 2017
Accepted 14 July 2017
Available online xxx

Keywords:

Dedifferentiation
Islets
VD3 treatment
MIN6
Vitamin D receptor

ABSTRACT

Dedifferentiation has been identified as one of the causes of β -cell failure resulting in type 2 diabetes (T2D). This study tested whether increasing vitamin D receptor (VDR) expression prevents dedifferentiation of β cells in a high-glucose state in vitro. Culturing a mouse insulinoma cell line (MIN6) in a high-glucose environment decreased VDR expression. However, increased VDR following vitamin D3 (VD3) treatment improved insulin release of early-passage MIN6 and insulin index of db/-(heterozygous) islets to levels seen in normal functional islets. Treatment with VD3, its analogues and derivatives also increased the expression of essential transcription factors, such as Pdx1, MafA and VDR itself, ultimately increasing expression of Ins1 and Ins2, which might protect β cells against dedifferentiation. VD3 agonist lithocholic acid (LCA) propionate was the most potent candidate molecule for protecting against dedifferentiation, and an e-pharmacophore mapping model confirmed that LCA propionate exhibits a stabilizing conformation within the VDR binding site. This study concluded that treating db/+ islets with a VD3 analogue and/or derivatives can increase VDR activity, preventing the pathological dedifferentiation of β cells and the onset of T2D.

© 2017 Elsevier Masson SAS. All rights reserved.

Introduction

Vitamin D (cholecalciferol) plays an essential role in human health and well-being. Cholecalciferol is the inactive form of vitamin D, generated in response to the absorption of light energy, that provides an important source for synthesis of $1\alpha,25$ -dihydroxyvi-

tamin D3 ($1,25[\text{OH}]_2\text{D}_3$) [1]. Humans can also access vitamin D through intakes of cholecalciferol, ergocalciferol (vitamin D2) and 25-hydroxycholecalciferol (25-hydroxyvitamin). Regardless of its source, once introduced into the body, vitamin D is transported to the liver where it is converted into 25-hydroxyvitamin D [2]. The amount of 25-hydroxyvitamin D in serum or plasma is indicative of the level of vitamin D in the body. Vitamin D that has been hydroxylated in the liver is transported in the bloodstream [3] and hydroxylated to $1,25[\text{OH}]_2\text{D}_3$, the active form of vitamin D, in the kidney [4,5]. This active form plays an important role in calcium homeostasis, and has an impact on functioning of the kidneys, intestines and bones [6]. It also has a known association with many non-calcaemic functions and some severe pathologies, such as cancer, obesity, autoimmune disorders and metabolic disorders, including type 1 (T1D) and type 2 diabetes (T2D).

Many of the effects of $1,25[\text{OH}]_2\text{D}_3$ are mediated after it interacts with the vitamin D receptor (VDR) [7], proven to exhibit non-classic actions that have three predominantly regulatory effects: secretion of hormones, immune function, and cell proliferation and differentiation [8]. VDR is a member of the nuclear hormone receptor superfamily, all of which have a

Abbreviations: MIN6, mouse insulinoma 6; VDR, vitamin D receptor; $1,25(\text{OH})_2\text{D}_3$, $1\alpha,25$ -dihydroxyvitamin D3; VDRE, vitamin D response element; CYP24A1, $1\alpha,25$ -dihydroxyvitamin D3 24-hydroxylase; DRIP, vitamin D receptor interacting protein; Ins1, insulin 1; Ins2, insulin 2; Glut2, glucose transporter 2; Pdx1, pancreas/duodenum homeobox protein 1; Oct-4, octamer-binding transcription factor 4; Pax-6, paired box 6; Gcg, glucagon; Gck, glucokinase; UCP2, uncoupling protein 2; MafA, v-maf avian musculoaponeurotic fibrosarcoma oncogene homologue F; LCA, lithocholic acid; p34/68/82, passage 34/68/82 cultured under high glucose concentrations for 34/68/82 generations; βCD , β -cell dedifferentiation; PBS, phosphate buffered saline; T2D, type 2 diabetes; $-/-$ mice, wild-type mice; db/ $-$ mice, heterozygous mice; db/db mice, homozygous mice.

* Corresponding author. Harry-Perkins Institute of Medical Research, Centre for Medical Research, University of Western Australia, Nedlands, Verdun St, Perth, 6009 Western Australia, Australia.

E-mail address: fang-xu.jiang@perkins.uwa.edu.au (F.-X. Jiang).

<http://dx.doi.org/10.1016/j.diabet.2017.07.006>

1262-3636/© 2017 Elsevier Masson SAS. All rights reserved.

Please cite this article in press as: Neelankal John A, et al. Vitamin D receptor-targeted treatment to prevent pathological dedifferentiation of pancreatic β cells under hyperglycaemic stress. Diabetes Metab (2017), <http://dx.doi.org/10.1016/j.diabet.2017.07.006>

conserved DNA-binding domain and a variable ligand-binding domain. Like other transcription factors, VDRs can only bind to six nucleotides residing within the major groove of DNA; these nucleotides form the consensus sequence of RGTSA (R = A/G, K = G/T, S = C/G) [9]. They can also be activated by a low nanomolar concentration of small lipophilic molecules [10]. Depending mainly on cell type, these nuclear receptors form either a heterodimer or homodimer. VDR achieves its nuclear function by binding with 1,25(OH)₂D₃ to form a transcription factor complex that later binds to vitamin D response elements (VDREs) within the promoter region of the target gene, thereby altering expression of the target gene within the cell [11].

Activation of VDREs within the promoter region results from heterodimerization of VDR with different types of retinoic acid receptors [12]. Activation of a gene by nuclear receptor is favoured by the interaction of the steroid receptor activation complex (SRC) [12] with the vitamin D receptor interacting protein (DRIP) complex [13], whereas repression is mediated by nuclear co-repressor (NCOR) dimerization with retinoic acid and thyroid receptors [14]. VDR binds to the co-repressor in the absence of 1,25(OH)₂D₃ and plays an important role in altering the expression of target genes. Any VD₃ entering cells is metabolized by activity of the cytochrome p450 superfamily of enzymes, including the important enzyme 1 α ,25-dihydroxyvitamin D₃ 24-hydroxylase (CYP24A1) [15].

Vitamin D plays a fundamental role in the release of insulin from pancreatic β cells, and an allelic variation in VDR can result in glucose intolerance and insulin sensitivity [16]. Previous studies have found that hypovitaminosis may be commonly observed in people with T2D. The role played by VDR in insulin release is governed by its presence in combination with vitamin D-dependent calcium-binding proteins in pancreatic tissue [17]. However, there remains a lack of understanding of the role VDR plays in the process of dedifferentiation.

β -cell dedifferentiation (BCD) results in a loss of function in pancreatic β cells [18]. Studies have assessed dedifferentiation in the mouse insulinoma cell line MIN6 exposed to high glucose concentrations for prolonged periods [19]. MIN6 responds to glucose challenges in a way similar to β cells [20]. Glucose is transported to pancreatic β cells by glucose transporter 2 (Glut2) protein [21], and pancreatic β cells release insulin in response to glucose levels. Insulin exocytosis from insulin granules is indicated by alterations in the ATP-to-ADP ratio within β cells. Synthesis of insulin in mouse islets derives from both insulin 1 (Ins1) and insulin 2 (Ins2) genes under the control of two major transcription factors: v-maf avian musculoaponeurotic fibrosarcoma oncogene homologue F (MafA) and pancreas/duodenum homeobox protein 1 (Pdx1) [22]. These have direct control over the expression of insulin genes by binding to promoters of these genes.

Dedifferentiation is also linked to increased expression of glucagon (Gcg) [18,19], and the expression of Gcg promoter increases when it binds to paired box 6 (Pax-6) protein [23]. Talchai et al. [24] concluded that dedifferentiation of β cells is a potential underlying cause of failure of pancreatic β cells in db/db mice. The leptin receptor modified db/db mouse model used in the study exhibited many classic characteristics of T2D, including hyperglycaemia, polyuria and glycosuria [25,26].

The objectives of the present study were to determine the effects of a high-glucose environment mimicking hyperglycaemia on VDRs and to monitor the effects of VD₃ treatment on β -cell function. The study also aimed to identify a compound that might potentially prevent β cells from undergoing dedifferentiation.

Materials and Methods

MIN6 culture

MIN6 cells were cultured in high-glucose (22.5 mM) Dulbecco's Modified Eagle Medium (DMEM) with 100 U/mL of penicillin, 100 μ g/mL of streptomycin, 10% fetal calf serum (FCS) and 1.5% HEPES in an incubator containing 10% CO₂ at 37°C. MIN6 cells passaged 32 times (p32) were cultured and then subcultured after 4 days until they reached p82. Cells from different passages were randomly selected and frozen in liquid nitrogen. Early and late passages were thawed and cultured for 48 h before each experimental procedure to acclimatize the cells to the optimal conditions.

RNA isolation and quantitative real-time polymerase chain reaction (RT-qPCR)

The TRIzol (Invitrogen Corporation, Carlsbad, CA, USA) method was used to extract total RNA. Cells were lysed by TRIzol reagent and the RNA-containing upper aqueous phase was separated from the lower organic phase. RNA in the upper aqueous phase was precipitated and washed with a 75% alcohol solution. Air-dried RNA pellets were dissolved in RNase/DNase-free water (Invitrogen) and the dissolved RNA concentration then quantified, using a NanoDrop ND-1000 spectrophotometer (Biolab Australia Pty Ltd, Melbourne, Victoria, Australia); 2000 ng of RNA (100 ng/ μ L) was then reverse-transcribed to generate cDNA in a reaction with a total volume of 20 μ L. The working standard for RT-qPCR was prepared by diluting 2 μ L of cDNA in 1000 μ L of RNase/DNase-free water. Paired primers were used to detect the genes for Ins1, Ins2, Glut2, Cyp24A1, Pdx1, Gck, UCP2, MafA and Gcg. RT-qPCR (Rotor-Gene Q, Qiagen, Hilden, Germany) was used to quantify the mRNA transcript using a KAPA SYBR Fast qPCR Master Mix (2 \times). The reaction process involved initial denaturation at 94°C for 5 min, 50 cycles of amplification with 30 s denaturation at 94°C, followed by 30 s annealing at 60°C and a final 30 s of extension at 72°C. Target transcripts were normalized to house-keeping gene Rps18 levels using Δ cycle threshold (Ct). Data were analyzed using the 2 $\Delta\Delta$ Ct method [27] (Table S1; see supplementary materials associated with this article online).

Flow cytometry

This was used to analyze protein expression in insulin. MIN6 cells were cultured until 90% confluence, then trypsinized and fixed with 4% paraformaldehyde (PFA). The fixed cells were permeabilized using BD Perm/Wash buffer (BD Biosciences, San Jose, CA, USA) to maximize permeabilization [28] before the addition of either APC-conjugated anti-mouse insulin (1:200, cat. no: 1C1417A; R&D Systems, Inc., Minneapolis, MN, USA) or VDR primary (1:100; cat. ab3508, Abcam, Inc., Cambridge, MA, USA). After 30 min of incubation, cells were washed, incubated for 30 min in secondary antibody for VDR (donkey anti-rabbit PE 1:800; cat. No. 12-4739, Affymetrix, Inc., Santa Clara, CA, USA) and counterstained with 4,6-diamidino-2-phenylindole (DAPI). The counterstained cells were then analyzed using a fluorescence-activated cell sorter (BD FACSAria II, BD Biosciences). Flow cytometry was optimized before performing the experiment. Levels of insulin expression were determined by identifying shifts in the peaks. The control for each experiment was done by exposure to only secondary antibody, thereby nullifying the effect of background staining. A significant change in the protein level under study was determined by monitoring shifts towards or away from the control. A shift of peak towards control indicated a reduction in protein level, whereas a shift of peak away from

control suggested an increase in protein. Analyses were performed in triplicate using 100,000 cells each.

Immunofluorescence analysis

MIN6 cells were cultured in sterile cover glass in high-glucose DMEM, containing 10% FCS, 2% penicillin/streptomycin and 1.5% HEPES, before being stored in an incubator containing 5% CO₂ at 37°C overnight. Then, the MIN6 cells adherent to the sterile cover glass were washed with phosphate-buffered saline (PBS), fixed in 4% PFA and permeabilized with 0.1% Triton X-100. The permeabilized cells were blocked with 10% donkey serum and exposed to primary antibody insulin or VDR antibody. Guinea-pig anti-mouse insulin antibody (1:200; ab7842, Abcam) and rat anti-mouse VDR (1:100; ab8756, Abcam) were used as primary antibodies, while Alexa Fluor 568 goat anti-guinea-pig antibodies (1:800; ab175714, Abcam) and goat anti-rat fluorescein isothiocyanate (FITC) antibodies (1:400; ab6840, Abcam) were used as secondary antibodies. The control for immunofluorescence analysis was performed using secondary antibody alone, and was carefully verified for background staining to avoid false-positive results. MIN6 cells were counterstained with DAPI, and images were captured under a Nikon microscope before being analyzed by specific software (NIS-Elements AR, 4.20.00 64 bit).

Transfection

VDR luciferase plasmids were obtained (from a colleague) with the luciferase gene under the control of VDR promoter [29]. The control plasmid used in the assay was Renilla luciferase. Both Renilla and VDR plasmids were separately transfected into NEB 5- α competent *E. coli*. The *E. coli* containing plasmids were cultured in LB agar containing 100 μ g/mL ampicillin, and one of the *E. coli* colonies was transferred to LB media (broth) and cultured overnight. Following overnight growth, the cultured plasmids were purified using a Plasmid Mini Kit (Qiagen). Both VDR luciferase and Renilla plasmids were then transfected into MIN6 cells using Lipofectamine LTX and PLUS reagents (Invitrogen), where they exhibited high transfection efficiency (80–90%).

MIN6 and VD3 treatment

Following dual transfection of MIN6 cells with VDR luciferase and Renilla plasmids, each passage was independently cultured under high- and low-glucose conditions. Some of the transfected cells were treated with chemicals, and a luciferase assay was then performed.

Luciferase assay

This assay was performed in accordance with the manufacturer's (Promega Corporation, Madison, WI, USA) protocol. The cultured MIN6 cells were washed with PBS, and the cells lysed using a lysis reagent (Dual-Luciferase Reporter Assay System, Promega). The 20 μ L cell lysate was mixed with 100 μ L of LAR II reagent, and luciferase activity was subsequently measured. To measure Renilla luciferase activity, 100 μ L of Stop & Glo Reagent (Promega) were added to the plate. The relative luciferase expression was calculated using Renilla.

Islet isolation

The use of mice (wild-type, db/+, db/db) was approved by the Animal Resources Centre Ethics Committee of Murdoch University (WIP 50). Islets were extracted from the pancreata of mice sacrificed by CO₂ asphyxiation at 12 weeks of age. Random blood

glucose levels in the wild-type mice were in the range of 8–8.5 mM, and 10–10.5 mM in the db/+ and 23–28 mM in the db/db mice. To isolate islets of Langerhans, the pancreas was perfused with a 3 mL collagenase P (1 IU/mL) solution dissolved in a Roswell Park Memorial Institute (RPMI) medium. The pancreata were digested and separated by density-gradient centrifugation.

Islet culture and treatment

Islets free of acinar cells after overnight incubation with 5% CO₂ were washed twice in RPMI-1066 and handpicked for treatment. Pure islets were incubated in RPMI-1066 with 100 U/mL of penicillin and 100 μ g/mL of streptomycin, 2 mM of glutamine and 10% FCS, along with VD3 analogues or derivatives. 1 α ,25-dihydroxyvitamin D₃, 22-oxacalcitriol (1 μ M), tacalcitol (1 μ M), lithocholic acid (LCA) acetate (6 μ M) and LCA propionate (6 μ M) were used as treatments, and each treatment was accompanied by control islets in RPMI medium containing penicillin/streptomycin, 10% FCS and 2 mM of glutamine. Controls and chemically treated islets were incubated at 37°C at a CO₂ concentration of 5% for 48 h.

Glucose-stimulated insulin secretion (GSIS) of treated MIN6

The MIN6 cell passages cultured and treated with different chemicals were washed with PBS and incubated with Krebs-Ringer buffer (KRB) (129 mM NaCl, 2.5 mM CaCl₂, 4.8 mM KCl, 5 mM NaHCO₃, 1.2 mM MgSO₄, 1.2 mM KH₂PO₄, 10 mM HEPES, 1 mg BSA/mL) for 1 h. Preincubated MIN6 cells as well as islets were incubated for 1 h at 37°C with a 5% CO₂ concentration in 200 μ L of KRB containing 2.75 mM (low-glucose challenge) or 22.5 mM (high-glucose challenge) of d-glucose. After 1 h of incubation, both the MIN6 cells and islets were centrifuged, and the supernatant removed and centrifuged again to remove any debris. The collected supernatant was used to perform an enzyme-linked immunosorbent assay (ELISA) to determine insulin levels (EMD Millipore, Billerica, MA, USA).

GSIS of islets

Five islets of uniform size from the control and each treatment were washed with PBS twice to remove any excess media before being used in the GSIS studies described above.

Acid-alcohol extraction of insulin from MIN6

After undergoing treatment with 1 α ,25-dihydroxyvitamin D₃, MIN6 cells were added to 500 μ L of acid-ethanol (1.5% HCL in 70% EtOH) and incubated overnight at –20°C. Supernatant was then removed and the procedure repeated, using 400 μ L of acid-ethanol to collect the total insulin contents. The supernatant pH was neutralized using Tris buffer (pH 7.5). The collected supernatants were diluted, and ELISA was performed. The total insulin contents were recorded in ng/mL with an appropriate dilution factor.

Statistical analyses

These were performed using one-way analysis of variance (ANOVA). A *P*-value < 0.05 was considered significant. One-way ANOVA with comparisons of selected pairs by Bonferroni post-hoc test was also performed.

Results

MIN6 cells were cultured in high-glucose DMEM (22.5 mM) for 4 days and then subcultured again, and samples from each passage

(p34, p48, p68 and p82) were frozen and stored. The stored frozen cells were later thawed for treatment with VD3 analogues and various derivatives. Each experiment was performed in triplicate using MIN6 cells that differed in terms of freeze/thaw cycles; statistical analyses were performed to nullify the effects of these cycles. The VD3, analogues and derivatives used to assess VDR-targeted therapy were tacalcitol (TC), oxacalcitriol (OC), LCA acetate and LCA propionate (Fig. 1). Optimal concentrations of each compound were predetermined using dose-response studies of MIN6. The basic structure of these VD3 derivatives and ligand molecules is formed by two core structures: carbon chains (C5–C6) linked by a cyclopentane ring; and a naphthalene-fused or alkenyl chain linked to a cyclohexane ring with an indane nucleus (Fig. 1). The structures of VD3, its analogues and derivatives were drawn using ChemDraw Ultra 8.0.3 software.

Reduced VDR expression may lead to dedifferentiation

In terms of morphological appearance, late-passage MIN6 cells display more projections, whereas early-passage MIN6 cells look spherical (Fig. 2A). Their VDR expression of RNA and protein levels is also different: RNA expression increased statistically significantly from early to later passages ($P = 0.02$; Fig. 2B). Levels of expression of the two insulin genes' (Ins1 and Ins2) mRNA levels were studied using qPCR, and comparative analyses revealed that these genes exhibited the same pattern of reduced insulin expression from early- to late-passage MIN6 cells with a significant value of $P < 1e-6$ (Fig. 2C). RNA expression of glucokinase (Gck) and uncoupling protein 2 (UCP2) decreased from p34 to p82 with P -values of 0.02 and 0.03, respectively (Fig. 2C). Immunofluorescence data reconfirmed that the level of insulin fell (Fig. 2D) from early to late passages and that the difference in insulin level was statistically significant ($P < 0.05$). Insulin protein expression in different passages was studied using immunofluorescence and fluorescence-activated cell-sorting (FACS; Fig. 2E), and the findings supported qPCR data.

Immunofluorescence studies of VDR protein (Fig. 2F) revealed a significant reduction in its expression between early and late

passages ($P = 0.005$). Different primer sequences were used to validate this RNA increase via qPCR. All primer pairs revealed that the increase in expression was statistically significant. FACS was later performed again to confirm the observation of immunofluorescence, and these data reconfirmed a reduction in VDR level from early to late passages (Fig. 2G), as indicated by a shift of peak away from control in p34 and a shift of peak towards control in the later passage.

$1\alpha,25$ -dihydroxyvitamin D₃-induced increase in insulin expression

The comparative analysis of VDR activity using luciferase assay between early and later passages showed a significant loss of VDR ($P = 0.00009$) on exposing MIN6 to high glucose levels for prolonged periods of time (Fig. 3A). The differential VDR activity of p34 MIN6 cells after treatment with 2.75 mM and 22.5 mM of glucose also showed a significant increase in VDR activity ($P = 0.0001$), whereas no differences in VDR activity were detected in later passages using different concentrations of glucose. VDR luciferase assay also revealed that VDR activity decreased from early to later passages when grown in high-glucose (22.5 mM) DMEM ($P = 0.00009$); however, no significant difference was observed between p34 and p82 when cells were cultured in low-glucose (2.75 mM) DMEM (Fig. 3B).

Luciferase assay was performed to study the effects of $1\alpha,25$ -dihydroxyvitamin D₃ ($1,25[\text{OH}]_2\text{D}_3$) on VDR activity. $1,25[\text{OH}]_2\text{D}_3$ was optimized at 10 mM (Fig. 3C), and the assay confirmed that TC, OC, LCA acetate and LCA propionate influenced VDR activity. Treating early-passage MIN6 cells with TC resulted in a statistically significant increase in VDR activity vs. $1,25[\text{OH}]_2\text{D}_3$ ($P = 0.02$). Treatment of MIN6 with the other molecules also had significant effects on induction of VDR activity with OC ($P = 0.00005$), LCA acetate ($P = 0.00001$) and LCA propionate ($P = 0.00007$). In addition, combination therapy had a statistically significant effect on VDR induction: for $1,25[\text{OH}]_2\text{D}_3$ with LCA acetate, the P -value was 0.00001, and $P = 0.00005$ with LCA propionate; $P = 0.0006$ for LCA propionate with TC; and $P < 1e-6$ for LCA propionate with OC (Fig. 3D). Further studies were

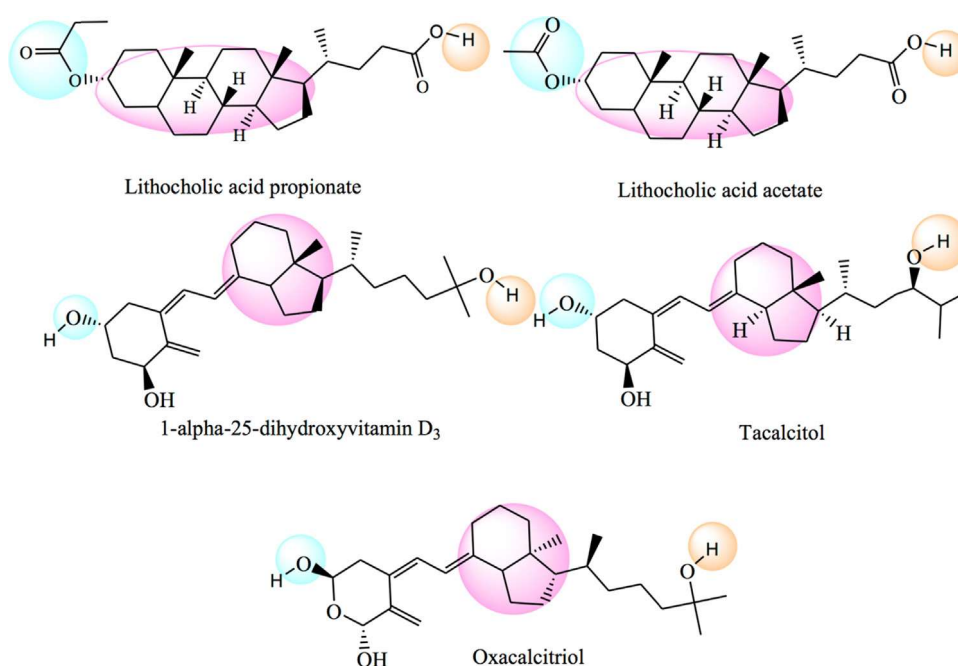


Fig. 1. Chemical structures of lithocholic acid (LCA) propionate, LCA acetate, $1\alpha,25$ -dihydroxyvitamin D₃, tacalcitol and oxacalcitriol. Blue indicates a hydrogen bond acceptor, pink indicates the lipophilic portion of the molecule and orange indicates a hydrogen bond donor.

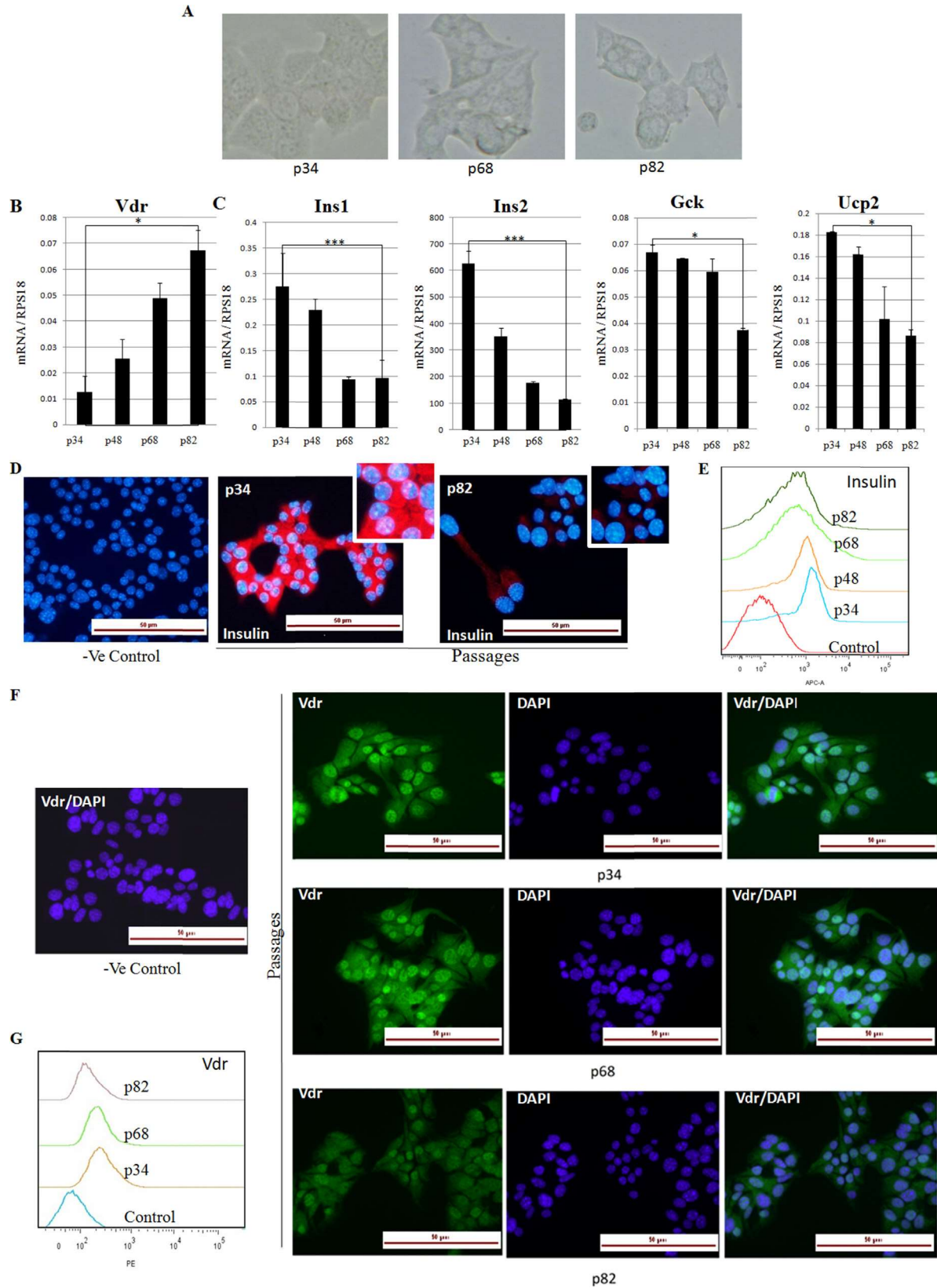


Fig. 2. (A) Vitamin D receptor (Vdr) analysis by quantitative polymerase chain reaction (qPCR) of different cell passages of MIN6 cultured in high-glucose media reveals significant differences between p34, p68 and p82. Gene expression of (B) Vdr and (C) insulin 1 (Ins1) and 2 (Ins2), glucokinase (Gck) and uncoupling protein 2 (Ucp2) by qPCR. (D) Insulin immunofluorescence shows insulin expression (red) and 4',6-diamidino-2-phenylindole (DAPI)-staining nuclei (blue). (E) Flow cytometry analysis for insulin (control has only secondary antibody). (F) Vdr immunofluorescence shows a decrease in protein expression from early to later passages: (left column) Vdr localization in MIN6 cell nuclei (green); (middle column) nuclease DAPI staining (blue); (right column) Vdr green overlapping DAPI staining, confirming Vdr localization in the nucleus. (G) Vdr flow cytometry shows a p34 shift away from control and a p82 shift towards control, indicating low Vdr protein expression in later passages.

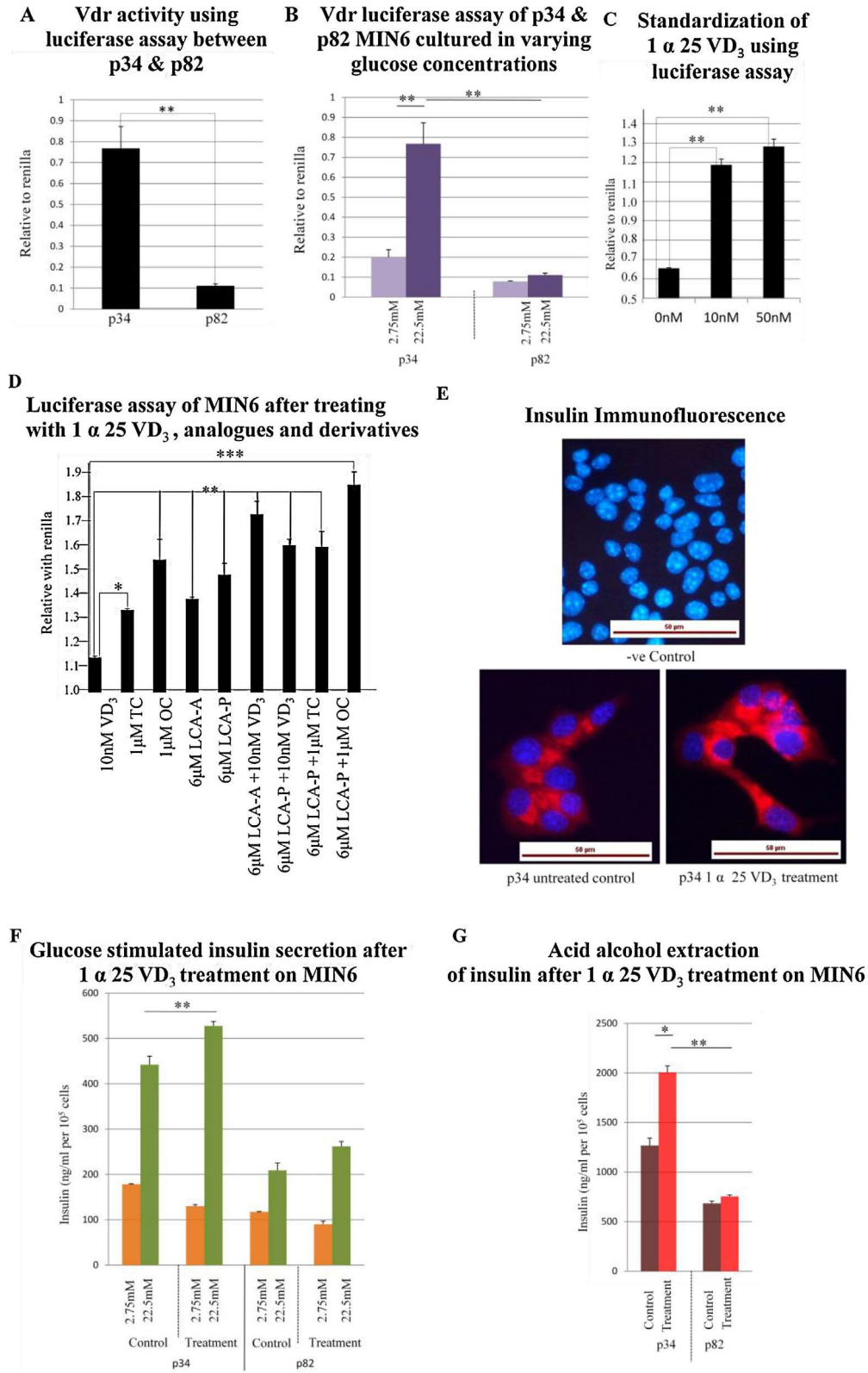


Fig. 3. Luciferase assay. A. Vitamin D receptor (Vdr) activity shows a significant reduction in the late passage. B. A significant increase in the early passage with differential glucose treatment. C. Effects with 1,25[OH]2D3 (1 α ,25-VD3) identifies 10 nM as optimal. D. Significant increases in Vdr expression following treatment with VD3, its derivatives and analogues. E. Immunohistochemistry analysis shows insulin levels (red) and DAPI-stained nuclei (blue). F. GIS of the early passage before and after VD3 treatment shows a significant increase, while the late passage shows the same pattern. G. There is a significant difference between control and treatment only in the early passage ($n = 3$; * $P < 0.05$; ** $P < 0.0001$; *** $P < 1e-6$).

performed after confirming these molecules had the potential to induce VDR activity.

Immunofluorescence of insulin revealed that the differences between the p34 control and treatment with 1,25[OH]2D3 were statistically significant ($P < 0.01$; Fig. 3E). Early and late passages of MIN6 cells before and after treatment with 1,25[OH]2D3 were used for GSIS. The high-glucose challenge after treatment with an active form of VD3 indicated that the differences in insulin release in untreated controls and treated samples were significant ($P = 0.0001$). Insulin release was reduced after treatment with 1,25[OH]2D3 in p34 in the low-glucose challenge, whereas the increase in insulin release in later passages after the high-glucose challenge was not statistically significant between the untreated controls and VD3-treated samples (Fig. 3F). The total quantity of insulin extracted from the MIN6 cells, using an acid–alcohol method, confirmed the significant difference in insulin contents with control vs 1,25[OH]2D3 treatment ($P = 0.02$). Late-passage MIN6 cells exhibited no differences between control and treated samples following acid–alcohol extraction, although there was a significant difference in insulin synthesis ($P < 0.0001$) between early and later passages (Fig. 3G).

VDR-mediated gene expression prevents dedifferentiation of β cells

qPCR was used to analyze gene expression in the various passages and to compare control with treatment samples. The insulin mRNA profile was determined according to Ins1 and Ins2 expression. Increases in Ins1 expression in p34 after treatment with 1,25[OH]2D3 and with LCA propionate were significant ($P = 0.0001$ and $P = 0.00005$, respectively), whereas there was no detectable difference before and after treatment with either 1,25[OH]2D3 or LCA propionate in p68 and p82 cells (Fig. 4A). Ins1 and Ins2 expression profiles were similar, while qPCR data indicated that treatment with 1,25[OH]2D3 and with LCA propionate had significant impacts on Ins2 expression ($P = 0.0007$ and $P = 0.00009$, respectively; Fig. 4B). However, no marked differences in Ins2 expression were observed in the latter two passages following treatment with either 1,25[OH]2D3 or LCA propionate vs untreated controls.

MafA mRNA was compared before and after treatment, and a significant difference was observed, and increases in MafA between controls and 1,25[OH]2D3 treatment were also statistically significant ($P = 0.05$), although increases with LCA propionate were considerably higher ($P = 0.03$; Fig. 4C). However, MafA expression differences between p68 and p82 or between control and treated samples were not statistically significant. Nevertheless, Pdx1 qPCR again detected a substantial increase with LCA propionate treatment ($P = 0.00006$) and an increase in expression with 1,25[OH]2D3 treatment ($P = 0.0001$). A broad pattern of increase in Pdx1 expression was also observed in the later p68 and p82 passages, although this was not statistically significant (Fig. 4D).

VDR mRNA expression increased following treatment with 1,25[OH]2D3 and LCA propionate; however, these differences were only significant in p34 cells. LCA propionate ($P = 2e-8$) and 1,25[OH]2D3 ($P = 0.001$) treatment significantly increased in comparison to untreated controls. VDR expression in later passages exhibited no statistically relevant differences following the various treatments (Fig. 4E).

The level of Gcg mRNA expression increased from early to later passages. After cells were treated with 1,25[OH]2D3 and LCA propionate, Gcg levels decreased in all passages, and a statistically significant decrease was observed in p82 ($P = 3e-9$ and $P = 0.001$ with 1,25[OH]2D3 and LCA propionate, respectively). Gcg expression was also significantly decreased in the p34

($P = 0.02$) and p82 ($P = 0.01$) passages after treatment with LCA propionate (Fig. 4F).

Effects of VDR-targeted treatments on wild-type heterozygous and db/db islets

GSIS was performed after treating islets isolated from wild-type mice with 1,25[OH]2D3, TC, OC, LCA acetate and LCA propionate. Glucose concentrations of 2.75 mM and 22.5 mM were used for the glucose challenge following the chemical treatments. The high-glucose challenge after any of the treated wild-type mouse islets vs untreated control islets showed no changes in insulin release (Fig. 5A). When the low- and high-glucose challenges were used to calculate the insulin index, they again showed no statistically significant differences between untreated controls and all five chemically treated islets (Fig. 5B).

However, there was a difference between treated and control prediabetic db/+ mouse islets in insulin release. Comparative analyses following the high-glucose challenge in db/+ control islets vs. active forms of VD3, analogues and derivatives exhibited a statistically significant difference across all treatments ($P < 0.0001$; Fig. 5C). Yet, even though the high-glucose challenge showed greater insulin release in treated vs untreated islets, most of the treatments were unable to convert this into an increase in insulin index. However, LCA acetate and LCA propionate both led to significant differences in insulin indices for control vs treated islets ($P = 0.00008$ and $P = 0.00001$, respectively; Fig. 5D). In fact, LCA propionate showed the highest insulin indices for db/+ islets with a range similar to those of the wild-type controls.

After purification by perfusion, diabetic homozygous db/db mouse islets were treated with active VD3 analogues and derivatives for 2 days before the GSIS challenges with low and high glucose levels. Compared with control islets, no significant differences were observed with high-glucose GSIS (Fig. 5E). However, insulin release after treating db/db islets with LCA acetate and LCA propionate revealed significant differences between low- and high-glucose states ($P < 0.01$), and the insulin increase (with high-glucose GSIS) after treatment with LCA acetate and LCA propionate was statistically significant vs. control ($P < 0.01$; Fig. 5F).

A comparative analysis of wild-type vs untreated db/+ control islets revealed that insulin release was significantly reduced in response to a high-glucose challenge ($P = 0.00004$), whereas a significant increase was observed after treating db/+ islets with LCA propionate ($P < 0.0001$). However, no significant differences in insulin release were observed between wild-type and db/+ mouse islets on glucose challenge (Fig. 5C), although significant increases were observed in the insulin index of untreated vs LCA propionate-treated islets ($P = 0.00008$; Fig. 5D).

Discussion

The present study aimed to assess whether chemical treatments can prevent the loss of β -cell function due to dedifferentiation. Culturing a MIN6 cell line model in high glucose for longer periods of time reduced VDR expression, whereas the increase in VDR observed on luciferase assay for each passage with low- and high-glucose levels suggests that cells have a VDR-controlled inbuilt mechanism that stabilizes β cells. The decrease in VDR expression from early to later passages could be due to a shortage of the VDR ligand VD3. In the absence of VD3, VDR remains inactive and fails to induce transcription of the VDR gene [30]. This might also explain the decrease of VDR in MIN6 cells during hyperglycaemia. Later passages of MIN6 presented with long cell-surface protrusions compared with early-passage cells. Indeed, previous

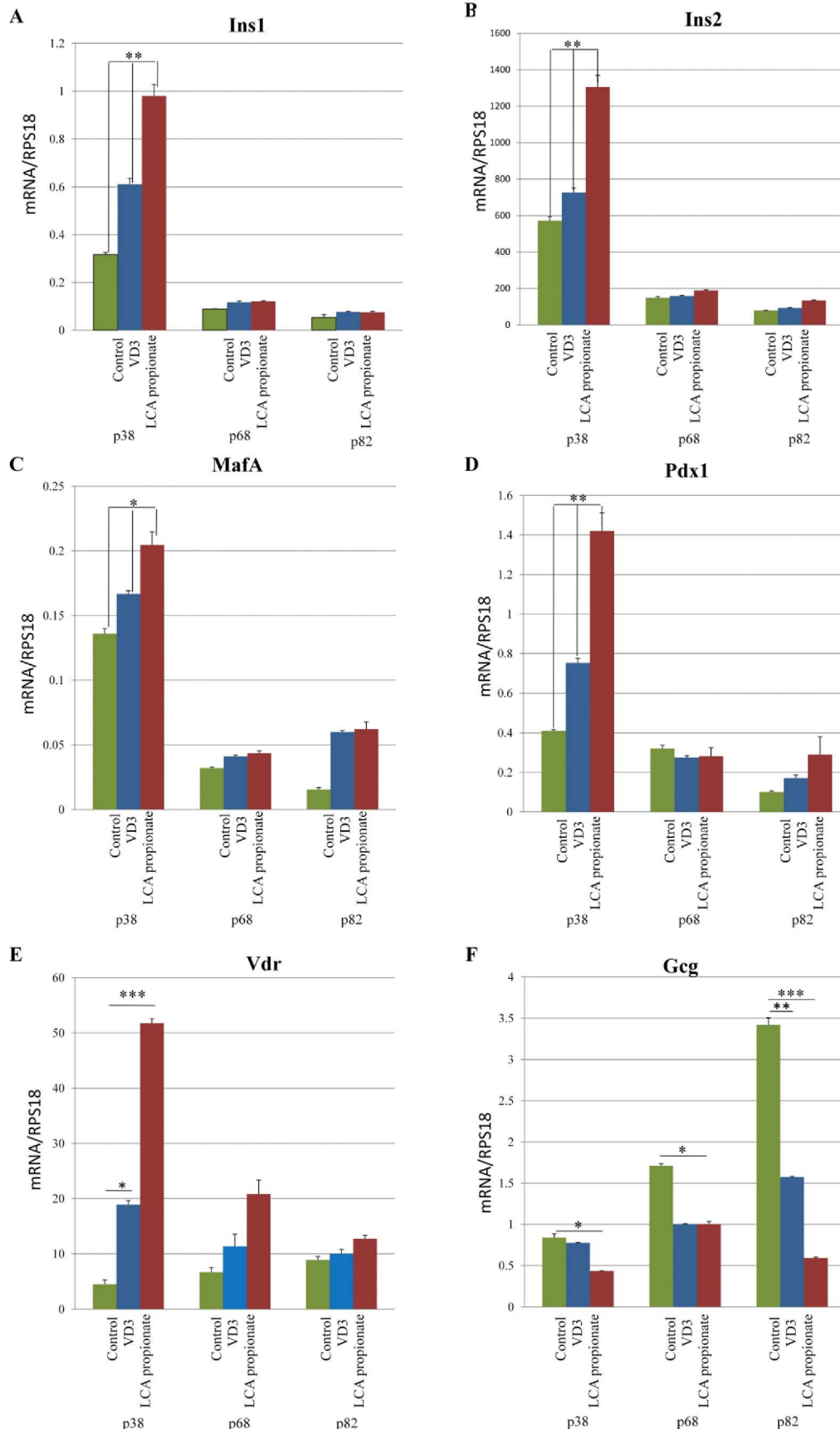


Fig. 4. Treatment with VD3 and LCA propionate shows (A) significant increases in Ins1 expression, but only the early passage, while (B) Ins2 gene expression, (C) MafA and (D) Pdx1 display similar patterns. (E) Vdr increases following LCA propionate treatment were highly significant in the early passage and also showed a pattern of increase across the later passages, whereas (F) the α -cell marker glucagon (Gcg) decreased in all passages, but the increases in p82 were particularly significant ($n = 3$; * $P < 0.05$; ** $P < 0.0001$; *** $P < 1e-6$).

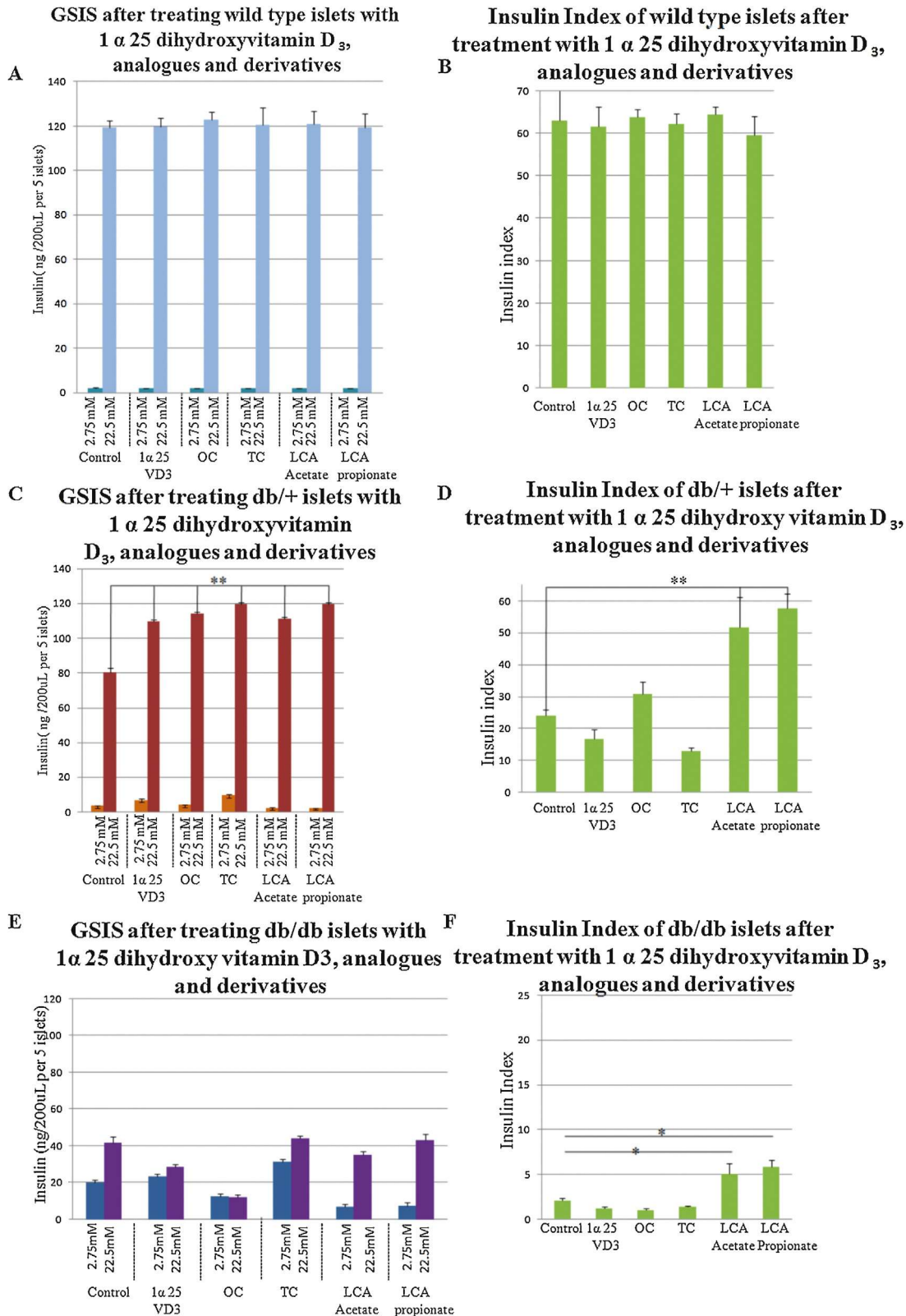


Fig. 5. (A) Glucose-stimulated insulin secretion (GSIS) in wild-type mouse islets shows no major differences between untreated control and treated islets, and (B) insulin indices are also similar, whereas (C) GSIS in db/+ mice shows significant differences between untreated controls and VD3-, analogue- and derivative-treated islets, with untreated islets significantly reduced vs. wild-type islets and significantly increased after treatment with LCA propionate vs. untreated islets. (D) Insulin indices in control and LCA acetate- and LCA propionate-treated db/+ islets are significantly increased, with the latter exhibiting the highest values in vitro. (E) GSIS in db/db islets after treatment show no increases in insulin release, whereas (F) treatment with LCA acetate and LCA propionate shows significant increases. OC: oxalacitriol; TC: tacialitol; LCA: lithocholic acid acetate (n = 3; * P < 0.05; ** P < 0.0001; *** P < 1e-6).

studies confirmed the presence of the neurological precursor gene in later passages, which may have caused the change in morphology of these cells [19].

In addition to such morphological differences, late-passage MIN6 cells have also shown a significant reduction in levels of the rate-limiting glycolytic enzyme Gck, thereby reducing levels of ATP, and it has been proven that a decreased ATP-to-ADP ratio in β cells reduces insulin secretion [31]. Another metabolic pathway implicated in β -cell dedifferentiation is mitochondrial dysfunction due to reduced expression of mitochondrial uncoupling protein 2 (UCP2). Pancreatic β cells express high levels of UCP2 which, in recent studies, have been found to be downregulated when levels of ATP are low [32]. The reduction in UCP2 impairs β -cell function due to oxidative stress [33]. UCP2 is upregulated by peroxisome proliferator-activated receptor (PPAR)- α [34] and repressed by forkhead box A1 (FOXA1) protein [35], which thus suggests possible roles for PPAR- α and FOXA1 in dedifferentiation. FOXO1 ablation is another mechanism recognized to cause dedifferentiation [24]. Cheng et al. [36] previously demonstrated that MIN6 loses glucose responsiveness, and is defective in glucose as well as lipid metabolism after prolonged culture in a high-glucose environment. A reduction in MIN6 insulin levels in a later passage may be due to dedifferentiation [19]. This reduction of VDR could be the potential cause of the low level of insulin expression and might play a vital role in dedifferentiation. Nevertheless, the role of VDR in pancreatic β -cell function is still currently not well understood. Zeitz et al. [37] postulated that a reduction in expression of vitamin D signalling might reduce the capacity of pancreatic β cells to respond to glucose challenges.

In contrast, the pattern of VDR interaction with 1,25[OH]2D3 (active VD3) has been well characterized [38,39]: it induces VDR in MIN6 cells and, thus, improves β -cell function while increasing the release of insulin in early vs late passages. Also, 1,25[OH]2D3 plays a modulatory role in the amount of insulin the islets release through the cyclic AMP pathway [40]. The improvement in function observed in later passages after treatment with VD3 was not as strong as that observed in earlier passages. A comparison of untreated and VD3-treated MIN6 revealed that cellular insulin levels were higher in treated vs untreated MIN6 cells, thereby suggesting that a VDR-VD3 complex plays an essential role in improving β -cell function as opposed to having a merely modulatory role in insulin release. Only a negligible increase in insulin was observed in later passages of MIN6 and was attributed to a significant reduction in VDR protein. The function of early-passage MIN6 cell function was similar to that of prediabetic β cells, whereas later passages exhibited characteristics similar to diabetic β cells [19]. VD3 treatment activates VDR into a functionally active transcription factor, which may have played an essential role in improving β -cell function in earlier passages. However, the dedifferentiated passage, which showed no similarities with dysfunctional islets isolated from diabetic mice, does not regain function with VD3 treatment. Further studies including chromatin immunoprecipitation sequencing (ChIP-seq) should now be performed to elucidate the precise mechanism through which VDR controls β -cell dedifferentiation.

VDR luciferase assay was used to analyze the potency of VD3 analogues and derivatives, and identified four different such compounds. The 1,25[OH]2D3 treatment of early MIN6 cell passages led to greater amounts of insulin than in untreated early passages. The newly identified VDR analogues and derivatives that can retain the maturity of pancreatic β cells are 22-OC, TC, LCA acetate and LCA propionate.

The mRNA expression of Pdx1 and MafA increased following LCA propionate treatment. These nuclear transcription factors are expressed in the early stage of development before being restricted later specifically to β cells [41]. Many previous studies of T2D

animal models have observed a reduction in levels of expression of Pdx1 following hyperglycaemia [42], and more recent studies have demonstrated that increased expression of Pdx1 and MafA can restore functionality in T2D patients [43]. Indeed, such increases after treatment may raise insulin synthesis, as increases in these two β -cell-specific transcription factors in early passages of MIN6 cells, representing the prediabetic condition, suggest that chemical treatments may play some sort of protective role. Analyses of markers of glucose metabolism (such as Gck) and of mitochondrial dysfunction may further reveal the potential role of LCA propionate in both processes. Both early and late passages exhibited decreases in progenitor marker genes and alpha-cell markers, which was also indicative of the role VDR plays in regaining the characteristics of β cells. Reduced levels of progenitor and alpha-cell markers, along with an increase in insulin following the induction of VDR as a nuclear transcription factor, present a plausible explanation of the role of VDR in maintaining pancreatic β -cell maturity.

The db/+ islets treated with VD3 analogues and derivatives increased expression of insulin, which supports the findings observed following treatment of MIN6 cells. These islets also showed diminished glucose responsiveness compared with wild-type islets, suggesting that those mice were in a prediabetic stage. Treating db/+ islets with VD3 analogues and derivatives, especially LCA acetate and LCA propionate, improved islet function. As patients with vitamin D deficiency (hypovitaminosis) have a greater propensity for T2D [44], such a susceptibility may be reduced by treatments with VD3 derivatives such as LCA acetate and LCA propionate. However, such derivatives and analogues, used to redifferentiate dedifferentiated db/db islets, had no effect on GSIS. As such, the present study indicates that loss of function cannot be restored by either VD3 or its analogues and derivatives. Nevertheless, the extent to which LCA acetate and LCA propionate were effective in preventing loss of β -cell function due to dedifferentiation indicates that these treatments may have some efficacy as a prediabetic drug therapy. The present study also found that LCA propionate was the most effective compound for protecting against dedifferentiation. Thus, these chemicals may yet play an important role in molecular medicine through their predictable pharmacokinetic and pharmacodynamic properties.

This study also evaluated the potential of vitamin D3 and its analogues as VDR agonists (VDRA), as these molecules bind to VDR and activate it to recruit cofactors to form transcriptional complexes that bind to VDREs in the promoter region of target genes [45]. This VDR ligand-binding plays a protective role in preventing loss of β -cell function following dedifferentiation. Our study has also established a pharmacophore model (modified from Nagamani et al. [46]) of a VDRA that can be exploited to increase its expression. Through the use of an e-pharmacophore mapping model, it may be postulated that pharmacophoric features should be present in chemical molecules to ensure their binding to VDR (Fig. 6I). To be a complete agonist of VDR, molecules must contain at least two hydrogen-bonding domains (a hydrogen bond donor and a hydrogen bond acceptor) and one hydrophobic domain (Fig. 6I). VDRA therapy seems more effective than native 1,25-dihydroxyvitamin D3 (calcitriol) derived from vitamin D supplementation as a mechanism for modulating β -cell differentiation. The relatively low potency of calcitriol, TC and OC to inhibit β -cell dedifferentiation may be attributed to only partial fulfilment of the proposed VDRA model. The flexibility and remote disposition of the alkenyl chain attached to the cyclohexane ring with an indane nucleus in relation to the carbon chains (C5-C6) are also of significance. In contrast, the enhanced VDR-protective capacity of LCA propionate by hampering dedifferentiation is due to complete fulfilment of the required VDRA model. In addition, LCA propionate and LCA acetate both carry the extra bulk of a decahydronaphthalene ring system, responsible for enhancing interaction with

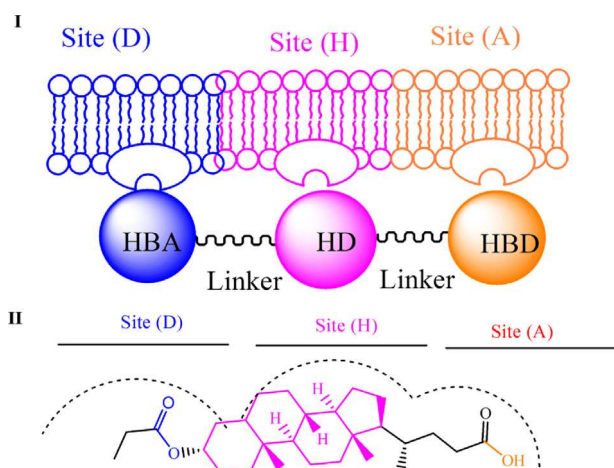


Fig. 6. (I) A proposed pharmacophore model for a vitamin D receptor agonist, modified from Nagamani et al. [46], depicts a hydrogen bond donor (HBD) and a hydrogen bond acceptor (HBA), separated by a hydrophobic domain (HD), all thought to interact with site (A). (II) The pharmacophore model for LCA propionate.

site H of the VDR (Fig. 6II), although LCA propionate demonstrates more promising agonist activity than LCA acetate, which might be attributed to the less-flexible ester linkage of the former vs the more flexible ester linkage of the latter.

Significant data from the literature therefore suggest that VDR is an essential transcription factor to prevent pancreatic β cells from undergoing dedifferentiation. One possible mechanism by which β cells are protected against dysfunction when under high-glucose stress is the increased activity of nuclear transcription factor VDR which, in turn, results in increased insulin synthesis and controlled insulin release. This increased activity of VDR can be positively regulated by a small new compound, designed and chemically synthesized as a complete VDRA with features identified by e-mapping. To develop further insight into the molecular mechanism(s) controlling dedifferentiation, ChIP-seq should also be performed. In the meantime, LCA propionate has been identified as an effective compound to protect pancreatic β cells from dedifferentiation under hyperglycaemic stress. An e-pharmacophore mapping model has also confirmed the potential of LCA propionate as a stabilizer in the VDR binding site. However, VD3 and its analogues and derivatives were found not to represent good therapeutic molecules for reversing T2D; instead, they could be used in prediabetes conditions to prevent loss of function and delay the onset of T2D.

Disclosure of interest

The authors declare that they have no competing interest.

Acknowledgements

We thank the Telethon-Perth Children's Hospital Research Fund and University of Western Australia for their financial support. We also thank for Diabetes Research WA for its support.

Appendix A. Supplementary data

Supplementary data associated with this article can be found, in the online version, at Supplementary materials (Table S1) associated with this article can be found at <http://www.sciencedirect.com> and <http://dx.doi.org/10.1016/j.diabet.2017.07.006>.

References

- [1] Holick MF. Vitamin D deficiency. *N Engl J Med* 2007;357:266–81.
- [2] Holick MF. Vitamin D: importance in the prevention of cancers, type 1 diabetes, heart disease and osteoporosis. *Am J Clin Nutr* 2004;79:362–71.
- [3] Chow EC, Durk MR, Maeng HJ, Pang KS. Comparative effects of 1 α -hydroxyvitamin D3 and 1,25-dihydroxyvitamin D3 on transporters and enzymes in *fxr(+)* and *fxr(-/-)* mice. *Biopharm Drug Dispos* 2013;34:402–16.
- [4] Chow EC, Sun H, Khan AA, Groothuis GM, Pang KS. Effects of 1 α , 25-dihydroxyvitamin D3 on transporters and enzymes of the rat intestine and kidney *in vivo*. *Biopharm Drug Dispos* 2010;31:91–108.
- [5] Calle C, Maestro B, Garcia-Arencibia M. Genomic actions of 1,25-dihydroxyvitamin D3 on insulin receptor gene expression, insulin receptor number and insulin activity in the kidney, liver and adipose tissue of streptozotocin-induced diabetic rats. *BMC Mol Biol* 2008;9:65.
- [6] Jurutka PW, Thompson PD, Whitfield GK, Eichhorst KR, Hall N, Dominguez CE, et al. Molecular and functional comparison of 1,25-dihydroxyvitamin D(3) and the novel vitamin D receptor ligand, lithocholic acid, in activating transcription of cytochrome P450 3A4. *J Cell Biochem* 2005;94:917–43.
- [7] Shaffer PL, Gewirth DT. Structural analysis of RXR-VDR interactions on DR3 DNA. *J Steroid Biochem Mol Biol* 2004;89-90:215–9.
- [8] Ozeki J, Choi M, Endo-Umeda K, Sakurai K, Amano S, Makishima M. Enhanced transcription of pancreatic peptide YY by 1 α -hydroxyvitamin D3 administration in streptozotocin-induced diabetic mice. *Neuropeptides* 2013;47:329–32.
- [9] Carlberg C, Bendik I, Wyss A, Meier E, Sturzenbecker LJ, Grippo JF, et al. Two nuclear signalling pathways for vitamin D. *Nature* 1993;361:657–60.
- [10] Yasmin R, Williams RM, Xu M, Noy N. Nuclear import of the retinoid X receptor, the vitamin D receptor and their mutual heterodimer. *J Biol Chem* 2005;280:40152–60.
- [11] Shaffer PL, Gewirth DT. Vitamin D receptor–DNA interactions. *Vitam Horm* 2004;68:257–73.
- [12] Koszewski NJ, Herberth J, Malluche HH. Retinoic acid receptor gamma 2 interactions with vitamin D response elements. *J Steroid Biochem Mol Biol* 2010;120:200–7.
- [13] Rachez C, Freedman LP. Mechanisms of gene regulation by vitamin D(3) receptor: a network of coactivator interactions. *Gene* 2000;246:9–21.
- [14] Orlov I, Rochel N, Moras D, Klaholz BP. Structure of the full human RXR/VDR nuclear receptor heterodimer complex with its DR3 target DNA. *EMBO J* 2012;31:291–300.
- [15] Sakaki T, Kagawa N, Yamamoto K, Inouye K. Metabolism of vitamin D3 by cytochromes P450. *Front Biosci* 2005;10:119–34.
- [16] Bid HK, Konwar R, Aggarwal CG, Gautam S, Saxena M, Nayak VL, et al. Vitamin D receptor (FokI, BsmI and TaqI) gene polymorphisms and type 2 diabetes mellitus: a North Indian study. *Indian J Med Sci* 2009;63:187–94.
- [17] Dupuis J, Langenberg C, Prokopenko I, Saxena R, Soranzo N, Jackson AU, et al. New genetic loci implicated in fasting glucose homeostasis and their impact on type 2 diabetes risk. *Nat Genet* 2010;42:105–16.
- [18] Cinti F, Bouchi R, Kim-Muller JY, Ohmura Y, Sandoval PR, Masini M, et al. Evidence of beta-cell dedifferentiation in human type 2 diabetes. *J Clin Endocrinol Metab* 2016;101:1044–54.
- [19] Neelankal John A, Morahan G, Jiang FX. Incomplete re-expression of neuroendocrine progenitor/stem cell markers is a key feature of beta-cell dedifferentiation. *J Neuroendocrinol* 2017;29.
- [20] Ishihara H, Asano T, Tsukuda K, Katagiri H, Inukai K, Anai M, et al. Pancreatic beta cell line MIN6 exhibits characteristics of glucose metabolism and glucose-stimulated insulin secretion similar to those of normal islets. *Diabetologia* 1993;36:1139–45.
- [21] Brown GK. Glucose transporters: structure, function and consequences of deficiency. *J Inher Metab Dis* 2000;23:237–46.
- [22] Deltour L, Vandamme J, Jouvenot Y, Duvill   B, Kelemen K, Schaerly P, et al. Differential expression and imprinting status of *Ins1* and *Ins2* genes in extraembryonic tissues of laboratory mice. *Gene Expr Patterns* 2004;5:297–300.
- [23] Ahmad Z, Rafeeq M, Collombat P, Mansouri A, et al. Pax6 inactivation in the adult pancreas reveals ghrelin as endocrine cell maturation marker. *PLoS One* 2015;10:e0144597.
- [24] Talchai C, Xuan S, Lin HV, Sussel L, Accili D, et al. Pancreatic beta cell dedifferentiation as a mechanism of diabetic beta cell failure. *Cell* 2012;150:1223–34.
- [25] Hummel KP, Dickie MM, Coleman DL. Diabetes, a new mutation in the mouse. *Science* 1966;153:1127–8.
- [26] Belke DD, Severson DL. Diabetes in mice with monogenic obesity: the *db/db* mouse and its use in the study of cardiac consequences. *Methods Mol Biol* 2012;933:47–57.
- [27] Livak KJ, Schmittgen TD. Analysis of relative gene expression data using real-time quantitative PCR and the 2^{(-Delta Delta C(T))} Method. *Methods* 2001;25:402–8.
- [28] Jiang FX, Li K, Archer M, Mehta M, Jamieson E, Charles A, et al. Differentiation of islet progenitors regulated by nicotinamide into transcriptome-verified beta cells that ameliorate diabetes. *Stem Cells* 2017;35:1341–54.
- [29] Jehan F, DeLuca HF. Cloning and characterization of the mouse vitamin D receptor promoter. *Proc Natl Acad Sci USA* 1997;94:10138–43.
- [30] Zella LA, Kim S, Shevde NK, Pike JW. Enhancers located within two introns of the vitamin D receptor gene mediate transcriptional autoregulation by 1,25-dihydroxyvitamin D3. *Mol Endocrinol* 2006;20:1231–47.

- [31] Liang Y, Bai G, Doliba N, Buettger C, Wang L, Berner DK, et al. Glucose metabolism and insulin release in mouse beta HC9 cells, as model for wild-type pancreatic beta-cells. *Am J Physiol* 1996;270:E846–57.
- [32] Chan CB, Kashemsant N. Regulation of insulin secretion by uncoupling protein. *Biochem Soc Trans* 2006;34:802–5.
- [33] Souza BM, Assmann TS, Kliemann LM, Gross JL, Canani LH, Crispim D. The role of uncoupling protein 2 (UCP2) on the development of type 2 diabetes mellitus and its chronic complications. *Arq Bras Endocrinol Metabol* 2011;55:239–48.
- [34] Tordjma K, Standley KN, Bernal-Mizrachi C, Leone TC, Coleman T, Kelly DP, et al. PPARAlpha suppresses insulin secretion and induces UCP2 in insulinoma cells. *J Lipid Res* 2002;43:936–43.
- [35] Vatamaniuk MZ, Gupta RK, Lantz KA, Doliba NM, Matschinsky FM, Kaestner KH, et al. Foxa1-deficient mice exhibit impaired insulin secretion due to uncoupled oxidative phosphorylation. *Diabetes* 2006;55:2730–6.
- [36] Cheng K, Delghingaro-Augusto V, Nolan CJ, Turner N, Hallahan N, Andrikopoulos S, et al. High passage MIN6 cells have impaired insulin secretion with impaired glucose and lipid oxidation. *PLoS One* 2012;7:e40868.
- [37] Zeitz U, Weber K, Soegiarto DW, Wolf E, Balling R, Erben RG. Impaired insulin secretory capacity in mice lacking a functional vitamin D receptor. *FASEB J* 2003;17:509–11.
- [38] Kato S, Kim MS, Yamaoka K, Fujiki R. Mechanisms of transcriptional repression by 1,25(OH)₂ vitamin D. *Curr Opin Nephrol Hypertens* 2007;16:297–304.
- [39] Jurutka PW, Whitfield GK, Hsieh JC, Thompson PD, Haussler CA, Haussler MR. Molecular nature of the vitamin D receptor and its role in regulation of gene expression. *Rev Endocr Metab Disord* 2001;2:203–16.
- [40] Bourlon PM, Faure-Dussert A, Billaudel B. Modulatory role of 1,25 dihydroxyvitamin D3 on pancreatic islet insulin release via the cyclic AMP pathway in the rat. *Br J Pharmacol* 1997;121:751–8.
- [41] Kaneto H, Miyatsuka T, Shiraiwa T, Yamamoto K, Kato K, Fujitani Y. Crucial role of PDX-1 in pancreas development, beta-cell differentiation and induction of surrogate beta-cells. *Curr Med Chem* 2007;14:1745–52.
- [42] Fujimoto K, Polonsky KS. Pdx1 and other factors that regulate pancreatic beta-cell survival. *Diabetes Obes Metab* 2009;4(11 Suppl):30–7.
- [43] Li F, Cao H, Sheng C, Sun H, Song K, Qu S. Upregulated Pdx1 and MafA contribute to beta-cell function improvement by sleeve gastrectomy. *Obes Surg* 2016;26:904–9.
- [44] Kostoglou-Athanassiou I, Athanassiou P, Gkountouvas A, Kaldrymides P, Vitamin D. and glycemic control in diabetes mellitus type 2. *Ther Adv Endocrinol Metab* 2013;4:122–8.
- [45] Matsuda S, Kitagishi Y. Peroxisome proliferator-activated receptor and vitamin d receptor signaling pathways in cancer cells. *Cancers (Basel)* 2013;5:1261–70.
- [46] Nagamani S, Kesavan C, Muthusamy K. E-Pharmacophore mapping and docking studies on Vitamin D receptor (VDR). *Bioinformation* 2012;8:705–10.